INORGANIC CHEMISTRY FRONTIERS

RESEARCH ARTICLE

View Article Online
View Journal | View Issue

Cite this: *Inorg. Chem. Front.*, 2025, **12**, 1295

Increasing excited state lifetimes of Cu(I) coordination complexes *via* strategic surface binding†

Jiaqi Chen,[a] Henry C. London,[a] Dhruba Pattadar,[b] Charlotte Worster,[c] Sahan R. Salpage,[a] Elena Jakubikova,*[c] S. Scott Saavedra*[b] and Kenneth Hanson*[a]

Received 24th September 2024,
Accepted 17th December 2024

DOI: 10.1039/d4qi02410a

rsc.li/frontiers-inorganic

Molecules undergo a structural change to minimize the energy of excited states generated *via* external stimuli such as light. This is particularly problematic for Cu(I) coordination complexes which are an intriguing alternative to the rare and expensive transition metal containing complexes (*e.g.*, Pt, Ir, Ru, *etc.*) but suffer from short excited state lifetimes due to D_{2d} to D_2 distortion and solvent coordination. Here we investigate strategic surface binding as an approach to hinder this distortion and increase the excited state lifetime of Cu(I) polypyridyl complexes. Using transient absorption spectroscopy, we observe a more than 20-fold increase in excited state lifetime, relative to solution, for a Cu(I) complex that can coordinate to the ZrO_2 *via* both carboxylated ligands. In contrast, the Cu(I) complex that coordinates *via* only one ligand has a less pronounced enhancement upon surface binding and exhibits greater sensitivity to coordinating solvents. A combination of ATR-IR and polarized visible ATR measurements as well as theoretical calculations suggest that the increased lifetime is due to surface binding which decreases the degrees of freedom for molecular distortion (*e.g.*, D_{2d} to D_2), with the doubly bound complex exhibiting the most pronounced enhancement.

Introduction

Molecules undergo a structural change to minimize the energy of transient excited states that are generated *via* external stimuli such as pressure, oxidants/reductants, magnetic fields, or light. This process is intrinsic to all molecules but large changes in structure, particularly of transition metal coordination complexes, can have a debilitating impact on their properties including decreased stability, lowered reactivity, and shortened excited state lifetimes.[1–4] This hinders their utility in catalysis, lighting, solar energy conversion, and more.[5,6] For example, in lighting/light harvesting applications, tetrahedral Cu(I) coordination complexes are an intriguing alternative to molecules containing expensive and low abundance transition metals like Ru(II), Pt(II), and Ir(III).[2] However, the lowest energy excited state of these Cu(I) complexes is typically dominated by metal-to-ligand charge transfer character where the resulting d^9, Cu(II) center favors a square planar geometry, resulting in a D_{2d} to D_2 distortion (Fig. 1).[7–9] This distortion decreases the energy of the excited states, enables access to additional relaxation modes, and opens sites for solvent coordination resulting in rapid, non-radiative decay.[10–13]

The most popular strategy to inhibit this type of distortion, particularly in the prototypical Cu(I) bis(1,10-phenanthroline) (phen) complexes, is *via* the addition of steric bulk to the ligands.[14] Increasing the size of the moiety at the 2,9-position from methyl groups (dmp) introduced by McMillin in the 1980s,[15] to phenyl,[16] *sec*-butyl,[17] cyclohexyl,[18] and *tert*-butyl,[19] has resulted in Cu(I) phen-based emitters with lifetimes >1 μs and emission quantum yields >5%, as compared 90 ns and

[a]*Department of Chemistry & Biochemistry, Florida State University, Tallahassee, Florida 32306, USA. E-mail: hanson@chem.fsu.edu*
[b]*Department of Chemistry & Biochemistry, University of Arizona, Tucson, Arizona, 85721, USA. E-mail: saavedra@arizona.edu*
[c]*Department of Chemistry, North Carolina State University, Raleigh, North Carolina, 27601, USA. E-mail: elena_jakubikova@ncsu.edu*

† Electronic supplementary information (ESI) available. See DOI: https://doi.org/10.1039/d4qi02410a

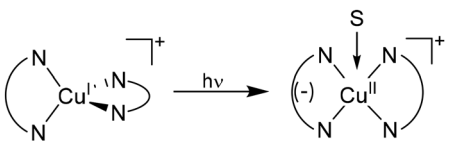

Fig. 1 General depiction of the tetrahedral to square planar (*i.e.*, D_{2d} to D_2) distortion in the excited state of Cu(I) polypyridyl complexes, and subsequent solvent (S) coordination.

0.4% for the parent $[Cu(dmp)_2]^+$.[15] While effective, this steric bulk strategy can suffer from limitations like increased synthetic complexity and decreased stability of the coordination sphere.[19] One can also hinder distortions by embedding the molecules in a rigid matrix or glass[20,21] but this strategy hinders mobility and access to the molecules for use in catalysis and photoinduced electron transfer.

Here, we introduce strategic surface binding as an alternative approach to hinder the distortion of Cu(I) polypyridyl complexes. We use metal ion-coordinating functional groups on the ligands to bind to a metal oxide substrate with the goal of hindering the D_{2d} to D_2-type distortion. We demonstrate that there is a >20-fold increase in excited state lifetime, relative to solution when both ligands are bound to the surface. This offers a new paradigm to extend the excited state lifetime of Cu(I) coordination complexes and hinder undesirable distortion pathways for molecules in response to stimuli.

Results and discussion

Synthesis and surface loading

The two Cu(I) complexes used for this study (**1** and **2**) are shown in Fig. 2. The 6,6′-dimethyl-2,2′-bipyridine scaffolding was selected, as opposed to the more common phenanthroline ligands, because of the relative ease of synthesizing COOH functionalized ligands.[22] The same or similar complexes were previously bound to metal oxide surfaces for application in dye-sensitized solar cells (DSSCs).[22] The position and number of ligands with the COOH functional groups were selected in such a way to allow only one (for **1**) or both (for **2**) ligands to bind to the metal oxide surface (Fig. 2; bottom).

Complexes **1** and **2** were prepared following previously published procedures.[22,23] Synthetic details and structural characterization are provided in the ESI.† Both **1** and **2** exhibits strong absorbance (Fig. 3a and Fig. S1†) from 250–350 nm and a weaker

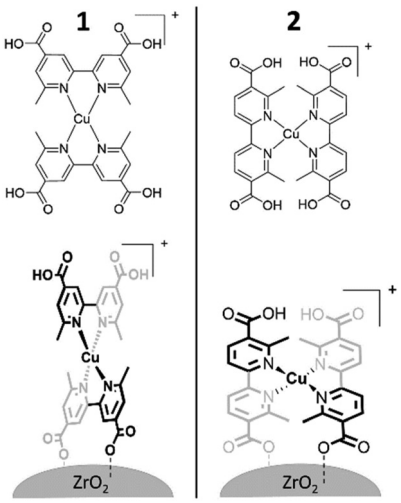

Fig. 2 Molecular structure (top) and envisioned ZrO_2 binding modes (bottom) for complexes **1** and **2**.

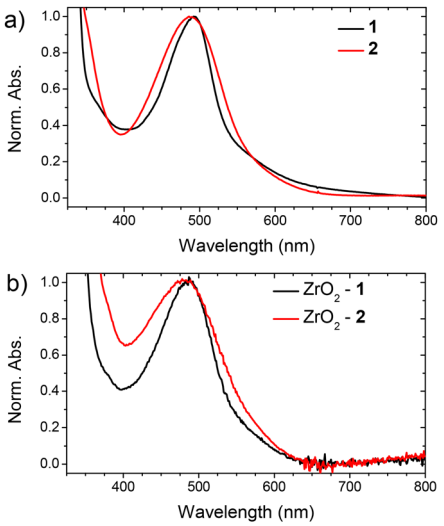

Fig. 3 Normalized absorption spectrum of **1** and **2** in MeOH (a) and on ZrO_2 (b).

feature at 400–600 nm that are attributed to π–π* and metal-to-ligand charge transfer (MLCT) transitions, respectively.[24]

The complexes were loaded onto the surface *via* soaking a ZrO_2 film in a 500 μM MeOH solution of **1** and **2**. The adsorption isotherms are provided in the ESI (Fig. S2†). As opposed to the more ubiquitous TiO_2, ZrO_2 was selected as the mesoporous oxide substrate[25] for these studies because its relatively high conduction band[26] allows for the excited state dynamics of the molecule to be studied in the absence of electron transfer quenching to the substrate. From fits to the absorption isotherms,[27] the complexes exhibit maximum surface coverages of 2.1×10^{-7} mol cm^{-2} for **1** and 3.6×10^{-8} mol cm^{-2} for **2**.

When bound to the surface (ZrO_2-**X**), the complexes maintain the same spectral features and energies, (Fig. 3b) albeit with peak broadening that is commonly attributed to inhomogeneous environments for molecules on metal oxide surfaces.[28] The lack of shift in the absorption energy/features suggests that the surface binding has minimal impact on energetics or protonation state, for example, and that the ground state structure of the molecule in solution is largely retained when bound to the surface.

Excited state dynamics

The excited-state dynamics of the Cu(I) complexes in MeOH and on ZrO_2 submerged in MeOH were measured by transient absorption (TA) spectroscopy and the results can be seen in Fig. 4. TA was chosen to monitor the excited state because the complexes were non-emissive even in rigid glass and at 77 K.

Upon 500 nm excitation, the complexes exhibit a bleach of the MLCT absorption band at <550 or 600 nm and an excited state absorption (ESA) feature at >550 or 600 nm, analogous to $[Cu(phen)_2]^+$ derivatives.[13] Worth noting is that the spectral features of **1** are redshifted relative to **2** (Fig. 4) presumably due to the 4,4′-, rather than 5,5′-position of the COOH groups, respectively, similar to the shift observed in ruthenium poly-

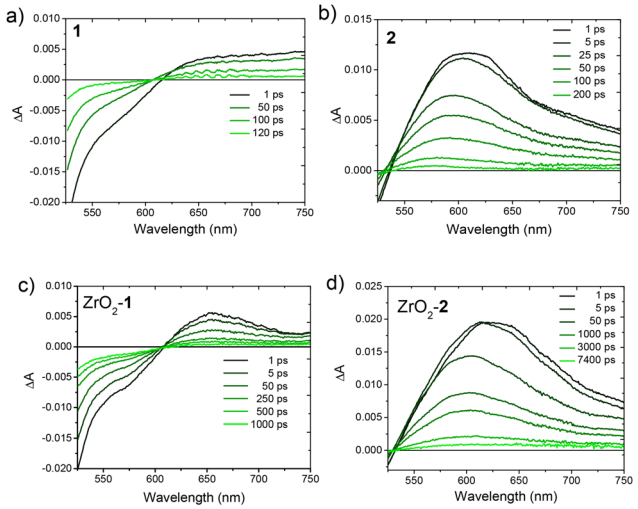

Fig. 4 Transient absorption spectra of complex **1** (a and c) and **2** (b and d) in MeOH (a and b) and on ZrO_2 in MeOH (c and d) (λ_{ex} = 500 nm).

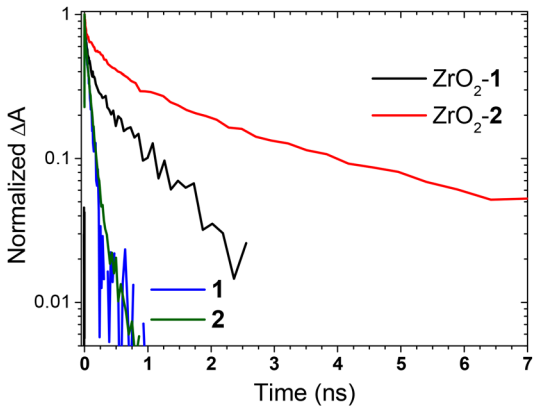

Fig. 5 Excited state decay traces for of **1** and **2** solvated and on ZrO_2 in MeOH at 690 nm and 610 nm, respectively (λ_{ex} = 500 nm).

Table 1 Excited state lifetime for solvated and surface bound complexes **1** and **2** in MeOH[a]

	τ in solution[b] (ps)	τ on ZrO_2 [c] (ps)	τ in PMMA[c,d] (ps)
1	80	640	2560
2	90	1960	4600

[a] Fits at 690 nm for **1** and 610 nm for **2**. [b] Single exponential fits. [c] Weighted average of biexponential fits. [d] The ethyl ester protected versions of the molecule ($\mathbf{1_{Et}}$ and $\mathbf{2_{Et}}$).

pridyl complexes.[29] For all the complexes in solution, at early time scales (<30 ps) there is a blueshift of the ESA feature (Fig. 4) that is often attributed to vibrational cooling.[30] In contrast, a more subtle blue shift occurs in ~500 ps for the surface bound complexes.

Comparing the solution and surface bound TA spectra, perhaps the most notable observation is the dramatic change in decay kinetics. Whereas the solution samples have returned to baseline in <300 ps, spectral features for the surface bound complexes are observed for several nanoseconds. Attempts to globally fit the decay kinetics using either sequential or parallel models were unsuccessful for the surface bound complexes (ZrO_2-**X**). This difficulty is not uncommon for these types of samples and again is attributed to inhomogeneous environments for molecules on metal oxide surfaces.[28] However, the single wavelength decay dynamics were fit with a single and biexponential function for solvated and ZrO_2 bound species, respectively (Table S1†). Regardless of wavelength, the biexponential fits to the ESA feature of ZrO_2-**X** samples (**X** = **1** or **2**) gave a consistent trend in both the fast (~50 and ~270 ps for **1** and **2**) and slow (~600 and ~2000 ps for **1** and **2**) components with approximately equal amplitude contribution for each (Table S1†). Given that the trends in decay were similar across ESA features (and across several independent samples), we chose representative wavelengths and weighted average lifetimes and the results are shown in Fig. 5 and Table 1, respectively.

When solvated in MeOH, the complexes exhibit excited state lifetimes <80 ps. In contrast, the lifetime for surface bound complexes is much longer and when compared solution, the lifetime increases ~8-fold for **1** and 22-fold for **2** (Table 1). Increased excited state lifetime for surface bound Cu(I) complexes has been observed before and was attributed to intermolecular packing hindering non-radiative distortions.[31] For the complexes studied here, the lifetimes did decrease when the surface loading was reduced by half (Fig. S3 and Table S2†), from 640 to 430 ps for **1** and 1960 to 1060 ps for **2** indicating the intermolecular interactions are not solely responsible for the lifetime increase. Instead, we attribute it to the surface binding decreasing excited state distortion of the complexes, and solvent coordination (*vida infra*), with the most pronounced behavior being complex **2** where both ligands are bound to the surface. For reference, we have included the excited state spectra (Fig. S4†) and lifetime (Table 1) for **1** and **2** in PMMA where the rigid matrix significantly hinders molecular mobility/flexibility.[32,33] Relative to the molecules in PMMA, ZrO_2-**2** more closely (43% of the PMMA lifetime) resembles that of the rigid environment than ZrO_2-**1** (25%).

As mentioned above, solvent coordination to the planarized, D_2 distorted Cu(I) complex can play a role in the excited state decay dynamics. Previous theoretical, time-resolved emission, and X-ray absorption studies on $[Cu(dmp)_2]^+$ derivatives, have indicated that structural distortion can occur on the subpicosecond timescale, followed by solvent coordination and relaxation on the 1–10 ps time scale.[7,34] MeOH was selected as the solvent of choice for the preliminary measurements due to the limited solubility and surface stability of **1** and **2** in other solvents. MeOH is known to serve as a coordinating Lewis Acid and excited state quencher for Cu(I) complexes.[35] Consequently, MeOH can serve as an indirect probe of the structural distortion that enables quenching *via* coordination.

To investigate the role of solvent in the excited state decay of solvated and surface bound Cu(I) complexes, we generated

the more soluble ethyl protected version of **1** and **2** ($\mathbf{1_{Et}}$ and $\mathbf{2_{Et}}$). As can be seen in Fig. S5 and 6,† the steady-state and time-resolved absorption spectral features of **1** and $\mathbf{1_{Et}}$, **2** and $\mathbf{2_{Et}}$ are similar. This indicates that other than increasing the solubility, the ethyl group has minimal impact on the photophysical properties of the complexes. The absorption and TA spectra (Fig. S7 and S8†) were measured in $CHCl_3$, the decay traces fit and theresults are summarized in Table 2.

For both $\mathbf{1_{Et}}$ and $\mathbf{2_{Et}}$, there is an ~40-fold increase in lifetime from MeOH to $CHCl_3$ which we attribute to the absence of excited state quenching *via* solvent coordination in $CHCl_3$.[35] Likewise, for ZrO_2-**1** there is a nearly 4-fold increase in lifetime in the non-coordinating $CHCl_3$. In contrast, for ZrO_2-**2** the lifetime slightly decreases from MeOH to $CHCl_3$ suggesting that the solvent dependent quenching mechanism for **2** in solution (*i.e.*, MeOH coordination) is significantly less prominent when it is bound to the surface. This outcome is consistent with inhibited D_{2d} to D_2 distortion for ZrO_2-**2** which hinders access for coordinating solvents to the metal center. Interestingly, the lifetime decrease for ZrO_2-**2** in $CHCl_3$ suggests that alternative non-radiative modes are available when bound to the surface.

Computational analysis

To gain insights into the electronic structure and degree of distortion upon excitation, we used density functional theory (DFT) (B3LYP,[36,37] SDD/6-311G*;[38,39] details in the ESI†) to optimize the geometries of compounds **1** and **2** in their singlet ground and lowest-energy triplet state. The ground state MO diagrams for the complexes are shown in Fig. 6 and Fig. S10.† Both complexes exhibit ligand-based LUMOs and Cu-based HOMOs (Fig. 6), where HOMO through HOMO−4 can be described as primarily metal centered, 3d orbitals (see Table S3†).

Using the ground state optimized geometry, the excited state transitions for **1** and **2** were then calculated using time-dependent density functional theory (TD-DFT) with the same model and the results are summarized in Tables S4 and 5† with the simulated spectrum shown in Fig. S12.† In agreement with experiment, the complexes exhibit strong, higher-energy peaks (<350 nm) that have ligand centered character (*i.e.*, π–π*) and lower-intensity peaks at ~500 nm that are MLCT in character. Transition dipole moments for the MLCT band were obtained from TD-DFT calculations and the results are summarized in Table S6† with the transition dipole moment vectors visualized in Fig. S13.† For both complexes, the MLCT transition dipoles are oriented from the metal center and bisect the bipyridine ligands. This orientation is consistent with previously reported Ru(II) and Os(II) tris-bipyridine complexes.[40,41] From the geometry optimized lowest-energy triplet state, **1** and **2** also exhibits MLCT character as confirmed by the spin density and natural orbital analysis (Fig. S14†).

Given our interest in the structural distortion of the complexes, we used the interligand dihedral angle (φ)[42] to evaluate the degree of planarization between the ground and lowest-energy ^{3}MLCT states (Table 3). The interligand dihedral angle (φ)[42] is the angle between planes of the bipyridine ligand (Fig. S11†). Note that since the complexes do not exhibit perfect D_{2d} symmetry, there are two different measurements of this angle, so the values reported in Table 3 correspond to their average. The φ = 90° corresponds to the tetrahedral structure, while φ = 0° or 180° describe a square planar structure. We have also calculated $\Delta\varphi = |90° - \varphi|$ that provides an information on deviation from tetrahedral conformation. The results are summarized in Table 3. For **1** and **2** we see flattening of the structure going from singlet to triplet state. The change is more pronounced for complex **2**, where the complex flattens by 9° going from singlet to triplet (this can be seen by comparing $\Delta\varphi$), and less apparent for complex **1** where it only flattens by additional 2°.

Collectively, the theoretical outcomes describe analogous behavior between **1** and **2** and prior Cu(I)(phen)$_2$ complexes.[15–19] Namely, excitation into a MLCT transition results in a ligand-centered reduction and oxidation of the Cu

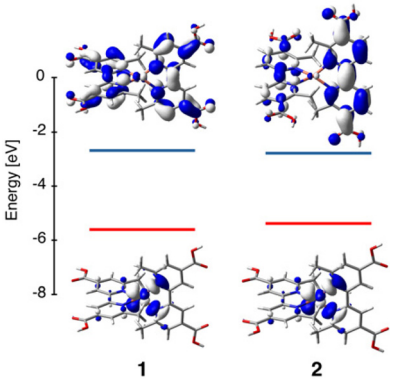

Fig. 6 Energy level diagrams for **1** and **2** with the HOMO (bottom, red line) and LUMO (top, blue line) orbitals.

Table 2 Excited state lifetime in MeOH and $CHCl_3$ for solvated $\mathbf{1_{Et}}$ and $\mathbf{2_{Et}}$ and ZrO_2 bound **1** and **2**

	τ in solution[a] (ps)			τ on ZrO_2 (ps)	
	In MeOH	In $CHCl_3$		In MeOH	In $CHCl_3$
$\mathbf{1_{Et}}$	70	2660	**1**	640	2420
$\mathbf{2_{Et}}$	55	2640	**2**	1960	1660

[a] For $\mathbf{1_{Et}}$ and $\mathbf{2_{Et}}$. From weighted average of biexponentail fits at 690 nm for ZrO_2-**1** and 610 nm for ZrO_2-**2**.

Table 3 Interligand dihedral angle (φ) and $\Delta\varphi = |90° - \varphi|$ for singlet ground state and triplet states of **1** and **2**

	Singlet		Triplet	
	φ	$\Delta\varphi$	φ	$\Delta\varphi$
1	81°	9°	101°	11°
2	74°	16°	65°	25°

(I) to Cu(II), which results in molecular distortion to a more square planar geometry (see Fig. 1). Our experimental results suggest that this process is inhibited by strategic surface binding.

Structural characterization

To gain insights into the structures of these interfaces we performed attenuated total reflectance infrared spectroscopy (ATR-IR) measurements on both the neat powders and ZrO_2 films of **1** and **2** and the results are shown in Fig. 7 and Fig. S15.†

In the neat powder, the complexes exhibit prominent peaks at 1715 cm^{-1} and 1700 cm^{-1} for **1** and **2**, respectively, that are assigned to the C=O stretching mode ($\nu_{C=O}$) and peaks at 1225–1245 cm^{-1} for the C–O stretching mode (ν_{C-O}).[43] The C=O stretching assignment is consistent with the calculated vibrational spectra (Fig. S16 and 17†) where the highest energy feature in the fingerprint region is the $\nu_{C=O}$ mode, along with a C–O stretch and O–H bands in the 1000–1700 cm^{-1} region. Upon binding to the surface, there is a notable decrease in the relative amplitude of the unbound $\nu_{C=O}$ and ν_{C-O} modes and an increase in the intensity of the carboxylate symmetric (ν_s) and asymmetric (ν_{as}) stretching in the 1600–1650 cm^{-1} region, which is attributed to surface binding.[43] It is important to note that while the amplitude of the unbound COOH modes decreases, they are still present in the surface bound samples. Given the geometric limitations of the molecules (*i.e.*, COOH groups on opposite sides), presumably, only half of the COOH groups are capable of binding to the surface and thus signal due to the unbound COOH groups is still observed.

Polarized UV-Vis attenuated total reflection (p-ATR) spectroscopy offers a powerful means of determining the orientation of molecular transition dipole moments relative to the surface normal.[44–47] Here we performed p-ATR on **1** and **2** bound to an indium tin oxide (ITO) surface and the results are summarized in Table 4 and Table S8† with the loading conditions shown in Table S7.† ITO was selected as the substrate because it is commercially available, has a low surface roughness (0.5 ± 0.1 nm), and the molecular orientation of absorbates is expected to be similar to that on ZrO_2.[48] In agreement with that observed for the ZrO_2 films (*vide supra*), the surface coverage was found to be similar between the complexes (~1 × 10^{-10} mol cm^{-2}). Assuming a hexagonal packing on a planar (*i.e.*, atomically flat) surface, this equates to a center-to-center intermolecular distance of ~15 Å,[46] which is in good agreement with full monolayers of related transition metal-polypyridyl complexes.[49]

Table 4 Transition dipole moment tilt angles and surface coverage of **1** and **2** on ITO as determined from p-ATR[a]

ITO-**X**	Tilt angle (°)	Surface coverage (mol cm^{-2})
1	47 ± 2	1.1×10^{-10} (±0.12)
2	62 ± 2	9.0×10^{-11} (±2.3)

[a] All values are the average of three measurements with the standard deviation reported as the relative error.

The tilt angle of the molecules was determined from the dichroic ratio (Fig. S18–20†) of the absorbance values measured using transverse magnetic and transverse electric polarized light at the MLCT transition (350–600 nm).[50] The complexes with carboxylic acid groups in the 5,5′ position of the bipyridine, **2** exhibited tilt angles of 62°. In contrast, for **1**, where the COOH groups are in the 4,4′ position, the tilt was 47° relative to surface normal.

Based on the combination of theoretical and experimental results described above, Fig. 8 shows the proposed orientation of the molecules on a metal oxide surface. The ground state optimized geometry of the complexes was oriented relative to the surface normal based on the calculated transition dipole moment and the p-ATR results. Based on the ATR-IR results, we assume that two of the four COOH groups of **1** and **2** were bound to the surface. These structures are consistent with the anticipated structure depicted in Fig. 2 and further support the hypothesis that in **1** only one of the ligands can bind, whereas in **2** both can bind which hinders the tetrahedral to square planar distortion.

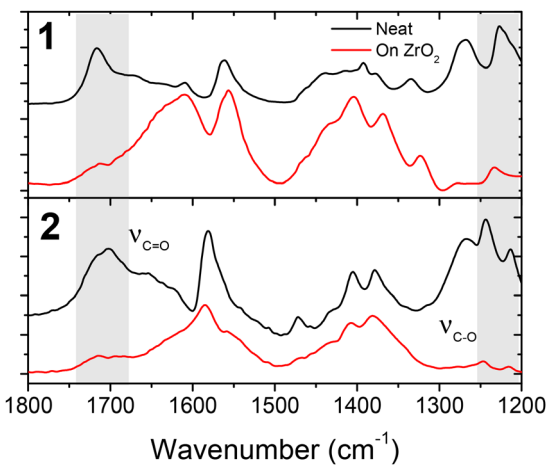

Fig. 7 ATR-IR absorption spectra of neat powder (black) and ZrO_2 bound (red) **1** and **2**.

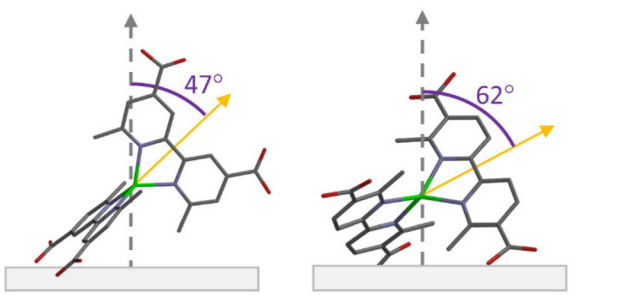

Fig. 8 Proposed structure of **1** (left) and **2** (right) on a metal oxide surface with the transition dipole moment in orange (H atoms omitted for clarity).

Conclusions

Here we studied the structural and excited state properties of two Cu(I) bipyridine complexes (*i.e.*, **1** and **2**) with variation in the position of the COOH surface binding group. Theoretical calculations for the complexes in solution point to a mechanism consisting of (1) excitation into a MLCT transition, (2) ligand-centered reduction and oxidation of the Cu(I) to Cu(II), and (3) molecular distortion from a tetrahedral to a square planar geometry. Upon ZrO_2 surface loading, ATR-IR and p-ATR measurements as well as geometric considerations indicate that molecules **1** are bound to the surface *via* a single ligand and molecule **2** coordinates *via* both carboxylated ligands. Using transient absorption, we observe a dramatic increase in the excited state lifetime for the molecules on a ZrO_2 surface, relative to solution, with the most pronounced increase for complex **2**. Furthermore, for **2** bound to the surface, the excited state quenching by a coordinating solvent like MeOH, was less pronounced than the singly bound derivative (*i.e.*, **1**) and it behaves more like that in a rigid matrix like PMMA. The increase in lifetime is not due to intermolecular interactions or energetic changes of the complex. Instead, we attribute it to surface binding decreasing the degrees of freedom for the molecules to distort with the doubly bound complex **2** having the greatest barrier to distortion. The hindered mobility decreases the excited state quenching *via* D_{2d} to D_2-type distortion and subsequent solvent coordination. Collectively, these results demonstrate that molecular immobilization *via* strategic surface binding is an alternative and innovative means of inhibiting undesired structural distortion for molecules responding to stimuli like light. However, it is important to acknowledge that the utility of these particular molecules is limited by their relatively short lifetime and non-emissive nature. But we hope these results will usher in a new paradigm for the design of molecule-metal oxide interfaces resulting in increased excited state lifetimes and efficiencies for light emission/harvesting applications as well as in electro-/photocatalysts where structural trapping at the interface could lead to coordinatively unsaturated sites and high energy species favorable for increased/unique reactivities.

Data availability

The data supporting this article have been included as part of the ESI.†

Conflicts of interest

There are no conflicts to declare.

Acknowledgements

Portions of this work were supported by the National Science Foundation under grant no. CHE-2246932. Structural characterization of the film was supported by the Army Research Office under grant no. W911NF-19-1-0357. Transient absorption measurements were performed on a spectrometer supported by the National Science Foundation under grant no. CHE-1919633. EJ and CW acknowledge support from the National Science Foundation under the grant no. CHE-1554855 as well as North Carolina State University, and the computing resources provided by North Carolina State University High Performance Computing Services Core Facility (RRID: SCR 022168). Some of the ATR data were acquired in the W.M. Keck Center for Nano-Scale Imaging in the Department of Chemistry and Biochemistry at the University of Arizona. This instrument was supported as part of the Center for Interface Science: Solar-Electric Materials (CIS: SEM), an Energy Frontier Research Center funded by the U.S. Department of Energy, Office of Science, Office of Basic Energy Sciences under Award No. DE-SC0001084.

References

1 J. K. McCusker, Electronic Structure in the Transition Metal Block and Its Implications for Light Harvesting, *Science*, 2019, **363**(6426), 484–488, DOI: **10.1126/science.aav9104**.
2 C. Wegeberg and O. S. Wenger, Luminescent First-Row Transition Metal Complexes, *JACS Au*, 2021, **1**(11), 1860–1876, DOI: **10.1021/jacsau.1c00353**.
3 P. C. Ford, From Curiosity to Applications. A Personal Perspective on Inorganic Photochemistry, *Chem. Sci.*, 2016, **7**(5), 2964–2986, DOI: **10.1039/C6SC00188B**.
4 B. C. Paulus, S. L. Adelman, L. L. Jamula and J. K. McCusker, Leveraging Excited-State Coherence for Synthetic Control of Ultrafast Dynamics, *Nature*, 2020, **582**(7811), 214–218, DOI: **10.1038/s41586-020-2353-2**.
5 C. K. Prier, D. A. Rankic and D. W. C. MacMillan, Visible Light Photoredox Catalysis with Transition Metal Complexes: Applications in Organic Synthesis, *Chem. Rev.*, 2013, **113**(7), 5322–5363, DOI: **10.1021/cr300503r**.
6 S. Ardo and G. J. Meyer, Photodriven Heterogeneous Charge Transfer with Transition-Metal Compounds Anchored to TiO_2 Semiconductor Surfaces, *Chem. Soc. Rev.*, 2009, **38**(1), 115–164, DOI: **10.1039/B804321N**.
7 N. A. Gothard, M. W. Mara, J. Huang, J. M. Szarko, B. Rolczynski, J. V. Lockard and L. X. Chen, Strong Steric Hindrance Effect on Excited State Structural Dynamics of Cu(I) Diimine Complexes, *J. Phys. Chem. A*, 2012, **116**(9), 1984–1992, DOI: **10.1021/jp211646p**.
8 A. Y. Kovalevsky, M. Gembicky and P. Coppens, Cu(I)(2,9-Bis(Trifluoromethyl)-1,10-Phenanthroline) 2+ Complexes: Correlation between Solid-State Structure and Photoluminescent Properties, *Inorg. Chem.*, 2004, **43**(26), 8282–8289, DOI: **10.1021/ic049638s**.
9 J. Huang, O. Buyukcakir, M. W. Mara, A. Coskun, N. M. Dimitrijevic, G. Barin, O. Kokhan, A. B. Stickrath, R. Ruppert, D. M. Tiede, J. F. Stoddart, J. P. Sauvage and

L. X. Chen, Highly Efficient Ultrafast Electron Injection from the Singlet MLCT Excited State of Copper(I) Diimine Complexes to TiO2 Nanoparticles, *Angew. Chem.,– Int. Ed.*, 2012, **51**(51), 12711–12715, DOI: 10.1002/anie.201204341.

10 D. R. McMillin, J. R. Kirchhoff and K. V. Goodwin, Exciplex Quenching of Photo-Excitd Copper Complexes, *Coord. Chem. Rev.*, 1985, **64**(C), 83–92, DOI: 10.1016/0010-8545(85)80043-6.

11 S. Garakyaraghi, E. O. Danilov, C. E. McCusker and F. N. Castellano, Transient Absorption Dynamics of Sterically Congested Cu(I) MLCT Excited States, *J. Phys. Chem. A*, 2015, **119**(13), 3181–3193, DOI: 10.1021/acs.jpca.5b00901.

12 M. Iwamura, S. Takeuchi and T. Tahara, Ultrafast Excited-State Dynamics of Copper(I) Complexes, *Acc. Chem. Res.*, 2015, **48**(3), 782–791, DOI: 10.1021/ar500353h.

13 G. B. Shaw, C. D. Grant, H. Shirota, E. W. Castner, G. J. Meyer and L. X. Chen, Ultrafast Structural Rearrangements in the MLCT Excited State for Copper(I) Bis-Phenanthrolines in Solution, *J. Am. Chem. Soc.*, 2007, **129**(7), 2147–2160, DOI: 10.1021/ja067271f.

14 G. Accorsi, A. Listorti, K. Yoosaf and N. Armaroli, 1,10-Phenanthrolines: Versatile Building Blocks for Luminescent Molecules, Materials and Metal Complexes, *Chem. Soc. Rev.*, 2009, **38**(6), 1690–1700, DOI: 10.1039/b806408n.

15 M. W. Blaskie and D. R. McMillin, Photostudies of Copper (I) Systems. 6. Room-Temperature Emission and Quenching Studies of Bis(2,9-Dimethyl-1,10-Phenanthroline)Copper(I), *Inorg. Chem.*, 1980, **19**(11), 3519–3522, DOI: 10.1021/ic50213a062.

16 C. T. Cunningham, K. L. H. Cunningham, J. F. Michalec and D. R. McMillin, Cooperative Substituent Effects on the Excited States of Copper Phenanthrolines, *Inorg. Chem.*, 1999, **38**(20), 4388–4392, DOI: 10.1021/ic9906611.

17 C. E. McCusker and F. N. Castellano, Design of a Long-Lifetime, Earth-Abundant, Aqueous Compatible Cu(I) Photosensitizer Using Cooperative Steric Effects, *Inorg. Chem.*, 2013, **52**(14), 8114–8120, DOI: 10.1021/ic401213p.

18 M. C. Rosko, K. A. Wells, C. E. Hauke and F. N. Castellano, Next Generation Cuprous Phenanthroline MLCT Photosensitizer Featuring Cyclohexyl Substituents, *Inorg. Chem.*, 2021, **60**(12), 8394–8403, DOI: 10.1021/acs.inorgchem.1c01242.

19 O. Green, B. A. Gandhi and J. N. Burstyn, Photophysical Characteristics and Reactivity of Bis(2,9-Di- *Tert* -Butyl-1,10-Phenanthroline)Copper(I), *Inorg. Chem.*, 2009, **48**(13), 5704–5714, DOI: 10.1021/ic802361q.

20 D. R. Corbin, D. F. Eaton and V. Ramamurthy, Modification of Photochemical Reactivity by Zeolites: Selective Photorearrangement of .Alpha.-Alkyldeoxybenzoins to p-Alkylbenzophenones in the Cavities of Faujasites, *J. Org. Chem.*, 1988, **53**(22), 5384–5386, DOI: 10.1021/jo00257a043.

21 T. Wu, J. Huang and Y. Yan, From Aggregation-Induced Emission to Organic Room Temperature Phosphorescence through Suppression of Molecular Vibration, *Cell Rep. Phys. Sci.*, 2022, **3**(2), 100771, DOI: 10.1016/j.xcrp.2022.100771.

22 E. C. Constable, A. H. Redondo, C. E. Housecroft, M. Neuburger and S. Schaffner, Copper(I) Complexes of 6,6′-Disubstituted 2,2′-Bipyridine Dicarboxylic Acids: New Complexes for Incorporation into Copper-Based Dye Sensitized Solar Cells (DSCs), *J. Chem. Soc., Dalton Trans.*, 2009, (No. 33), 6634–6644, DOI: 10.1039/b901346f.

23 B. Bozic-Weber, E. C. Constable, C. E. Housecroft, M. Neuburger and J. R. Price, Sticky Complexes: Carboxylic Acid-Functionalized N-Phenylpyridin-2- Ylmethanimine Ligands as Anchoring Domains for Copper and Ruthenium Dye-Sensitized Solar Cells, *Dalton Trans.*, 2010, **39**(15), 3585–3594, DOI: 10.1039/b925623g.

24 V. Leandri, A. R. P. Pizzichetti, B. Xu, D. Franchi, W. Zhang, I. Benesperi, M. Freitag, L. Sun, L. Kloo and J. M. Gardner, Exploring the Optical and Electrochemical Properties of Homoleptic versus Heteroleptic Diimine Copper(I) Complexes, *Inorg. Chem.*, 2019, **58**(18), 12167–12177, DOI: 10.1021/acs.inorgchem.9b01487.

25 J. C. Wang, K. Violette, O. O. Ogunsolu, S. Cekli, E. Lambers, H. M. Fares and K. Hanson, Self-Assembled Bilayers on Nanocrystalline Metal Oxides: Exploring the Non-Innocent Nature of the Linking Ions, *Langmuir*, 2017, **33**(38), 9609–9619, DOI: 10.1021/acs.langmuir.7b01964.

26 R. Katoh, A. Furube, T. Yoshihara, K. Hara, G. Fujihashi, S. Takano, S. Murata, H. Arakawa and M. Tachiya, Efficiencies of Electron Injection from Excited N3 Dye into Nanocrystalline Semiconductor (ZrO_2, TiO_2, ZnO, Nb_2O_5, SnO_2, In_2O_3) Films, *J. Phys. Chem. B*, 2004, **108**(15), 4818–4822, DOI: 10.1021/jp031260g.

27 I. Langmuir, THE ADSORPTION OF GASES ON PLANE SURFACES OF GLASS, MICA AND PLATINUM, *J. Am. Chem. Soc.*, 1918, **40**(9), 1361–1403, DOI: 10.1021/ja02242a004.

28 J. R. Durrant, S. A. Haque and E. Palomares, Towards Optimisation of Electron Transfer Processes in Dye Sensitised Solar Cells, *Coord. Chem. Rev.*, 2004, **248**(13–14), 1247–1257, DOI: 10.1016/j.ccr.2004.03.014.

29 H. Zabri, I. Gillaizeau, C. A. Bignozzi, S. Caramori, M.-F. Charlot, J. Cano-Boquera and F. Odobel, Synthesis and Comprehensive Characterizations of New *Cis* -RuL_2X_2 (X = Cl, CN, and NCS) Sensitizers for Nanocrystalline TiO_2 Solar Cell Using Bis-Phosphonated Bipyridine Ligands (L), *Inorg. Chem.*, 2003, **42**(21), 6655–6666, DOI: 10.1021/ic034403m.

30 L. X. Chen, G. B. Shaw, I. Novozhilova, T. Liu, G. Jennings, K. Attenkofer, G. J. Meyer and P. Coppens, MLCT State Structure and Dynamics of a Copper(I) Diimine Complex Characterized by Pump–Probe X-Ray and Laser Spectroscopies and DFT Calculations, *J. Am. Chem. Soc.*, 2003, **125**(23), 7022–7034, DOI: 10.1021/ja0294663.

31 M. S. Eberhart, B. T. Phelan, J. Niklas, E. A. Sprague-Klein, D. M. Kaphan, D. J. Gosztola, L. X. Chen, D. M. Tiede, O. G. Poluektov and K. L. Mulfort, Surface Immobilized Copper(I) Diimine Photosensitizers as Molecular Probes for Elucidating the Effects of Confinement at Interfaces for Solar Energy Conversion, *Chem. Commun.*, 2020, **56**(81), 12130–12133, DOI: 10.1039/D0CC05972B.

32 F. Wu, H. Tong, K. Wang, Z. Wang, Z. Li, X. Zhu, W.-Y. Wong and W.-K. Wong, Synthesis, Structural Characterization and Photophysical Studies of Luminescent Cu(I) Heteroleptic Complexes Based on Dipyridylamine, *J. Photochem. Photobiol., A*, 2016, **318**, 97–103, DOI: 10.1016/j.jphotochem.2015.12.003.

33 D. Felder, J.-F. Nierengarten, F. Barigelletti, B. Ventura and N. Armaroli, Highly Luminescent Cu(I)–Phenanthroline Complexes in Rigid Matrix and Temperature Dependence of the Photophysical Properties, *J. Am. Chem. Soc.*, 2001, **123**(26), 6291–6299, DOI: 10.1021/ja0043439.

34 G. Levi, E. Biasin, A. O. Dohn and H. Jónsson, On the Interplay of Solvent and Conformational Effects in Simulated Excited-State Dynamics of a Copper Phenanthroline Photosensitizer, *Phys. Chem. Chem. Phys.*, 2020, **22**(2), 748–757, DOI: 10.1039/c9cp06086c.

35 C. O. Dietrich-Buchecker, P. A. Marnot, J. P. Sauvage, J. R. Kirchhoff and D. R. McMillin, Bis(2,9-Diphenyl-1,10-Phenanthroline)Copper(I): A Copper Complex with a Long-Lived Charge-Transfer Excited State, *J. Chem. Soc. – Series Chem. Commun.*, 1983, (No. 9), 513–515, DOI: 10.1039/C39830000513.

36 A. D. Becke, Density-Functional Exchange-Energy Approximation with Correct Asymptotic Behavior, *Phys. Rev. A*, 1988, **38**(6), 3098–3100, DOI: 10.1103/PhysRevA.38.3098.

37 S. Grimme, Semiempirical GGA-Type Density Functional Constructed with a Long-Range Dispersion Correction, *J. Comput. Chem.*, 2006, **27**(15), 1787–1799, DOI: 10.1002/jcc.20495.

38 M. Dolg, U. Wedig, H. Stoll and H. Preuss, Energy–adjusted Ab Initio Pseudopotentials for the First Row Transition Elements, *J. Chem. Phys.*, 1987, **86**(2), 866–872, DOI: 10.1063/1.452288.

39 L. Yang, D. R. Powell and R. P. Houser, Structural Variation in Copper(I) Complexes with Pyridylmethylamide Ligands: Structural Analysis with a New Four-Coordinate Geometry Index, τ_4, *Dalton Trans.*, 2007, (No. 9), 955–964, DOI: 10.1039/B617136B.

40 K. Kawamoto, Y. Tamiya, T. Storr, R. J. Cogdell, I. Kinoshita and H. Hashimoto, Disentangling the 1MLCT Transition of [Ru(Bpy)3]2+ by Stark Absorption Spectroscopy, *J. Photochem. Photobiol., A*, 2018, **353**, 618–624, DOI: 10.1016/j.jphotochem.2017.08.025.

41 E. M. Kober and T. J. Meyer, Concerning the Absorption Spectra of the Ions M(Bpy)32+ (M = Fe, Ru, Os; Bpy = 2,2′-Bipyridine), *Inorg. Chem.*, 1982, **21**(11), 3967–3977, DOI: 10.1021/ic00141a021.

42 L. Du and Z. Lan, Ultrafast Structural Flattening Motion in Photoinduced Excited State Dynamics of a Bis(Diimine) Copper(I) Complex, *Phys. Chem. Chem. Phys.*, 2016, **18**(11), 7641–7650, DOI: 10.1039/C5CP06861D.

43 Y. Bai, I. Mora-Seró, F. De Angelis, J. Bisquert and P. Wang, Titanium Dioxide Nanomaterials for Photovoltaic Applications, *Chem. Rev.*, 2014, **114**(19), 10095–10130, DOI: 10.1021/cr400606n.

44 H.-C. Lin, G. A. MacDonald, Y. Shi, N. W. Polaske, D. V. McGrath, S. R. Marder, N. R. Armstrong, E. L. Ratcliff and S. S. Saavedra, Influence of Molecular Orientation on Charge-Transfer Processes at Phthalocyanine/Metal Oxide Interfaces and Relationship to Organic Photovoltaic Performance, *J. Phys. Chem. C*, 2015, **119**(19), 10304–10313, DOI: 10.1021/acs.jpcc.5b02971.

45 L. E. Oquendo, R. Ehamparam, N. R. Armstrong, S. S. Saavedra and D. V. McGrath, Zinc Phthalocyanine–Phosphonic Acid Monolayers on ITO: Influence of Molecular Orientation, Aggregation, and Tunneling Distance on Charge-Transfer Kinetics, *J. Phys. Chem. C*, 2019, **123**(12), 6970–6980, DOI: 10.1021/acs.jpcc.8b10301.

46 A. Arcidiacono, Y. Zhou, W. Zhang, J. O. Ellison, S. Ayad, E. S. Knorr, A. N. Peters, L. Zheng, W. Yang, S. S. Saavedra and K. Hanson, Examining the Influence of Bilayer Structure on Energy Transfer and Molecular Photon Upconversion in Metal Ion Linked Multilayers, *J. Phys. Chem. C*, 2020, **124**(43), 23597–23610, DOI: 10.1021/acs.jpcc.0c08715.

47 D. Pattadar, A. Arcidiacono, D. Beery, K. Hanson and S. S. Saavedra, Molecular Orientation and Energy Transfer Dynamics of a Metal Oxide Bound Self-Assembled Trilayer, *Langmuir*, 2023, **39**(30), 10670–10679, DOI: 10.1021/acs.langmuir.3c01323.

48 D. Pattadar, L. Zheng, A. J. Robb, D. Beery, W. Yang, K. Hanson and S. S. Saavedra, Molecular Orientation of $-PO_3H_2$ and $-COOH$ Functionalized Dyes on TiO_2, Al_2O_3, ZrO_2, and ITO: A Comparative Study, *J. Phys. Chem. C*, 2023, **127**(5), 2705–2715, DOI: 10.1021/acs.jpcc.2c08632.

49 T. C. Motley, M. D. Brady and G. J. Meyer, Influence of 4 and 4′ Substituents on $Ru^{III/II}$ Bipyridyl Self-Exchange Electron Transfer Across Nanocrystalline TiO_2 Surfaces, *J. Phys. Chem. C*, 2018, **122**(34), 19385–19394, DOI: 10.1021/acs.jpcc.8b05281.

50 S. B. Mendes, J. T. Bradshaw and S. S. Saavedra, Technique for Determining the Angular Orientation of Molecules Bound to the Surface of an Arbitrary Planar Optical Waveguide, *Appl. Opt.*, 2004, **43**(1), 70, DOI: 10.1364/AO.43.000070.

